J Biomol NMR (2013) 57:369–374
DOI 10.1007/s10858-013-9797-8

NMR STRUCTURE NOTE

# Solution structure of a putative FKBP-type peptidyl-propyl *cis–trans* isomerase from *Giardia lamblia*

**Garry W. Buchko · Stephen N. Hewitt · Wesley C. Van Voorhis · Peter J. Myler**

Received: 12 November 2013 / Accepted: 19 November 2013 / Published online: 29 November 2013


## Biological content

The FK506 Binding Protein (FKBP) super-family was named for the ability of these proteins to bind to the immunosuppressive drug FK506, a 23-member macrolide lactone. Immunosuppression is achieved when the protein-FK506 complex binds to calcineurin to form a larger complex that blocks signal transduction in the T-lymphocyte transduction pathway (Göthel and Marahiel 1999). FKBP proteins also have peptidyl-proline *cis–trans* isomerases (PPIase) activity that catalyzes the interconversion of the peptidyl-prolyl imide bond between the *cis* and *trans* configuration in peptide and protein substrates (Göthel and Marahiel 1999). The isomerase activity is unrelated to the immunosuppressive effects when bound to FK506, but, is essential for the proper folding of many proteins and a number of PPIases act as chaperones. Because proper protein folding is often necessary for proper biochemical function, FKBP proteins are indirectly associated with many diverse biologically processes including trafficking, cell-cycle regulation, development, and signal transduction (Göthel and Marahiel 1999). It has been observed that the parasite *Trypanosoma cruzi* secretes a FKBP-type protein upon infecting its host, leading to the suggestion that some parasites may use these proteins as virulence factors (Moro et al. 1995). Cultures of the parasite responsible for malaria, *Plasmodium falciparum*, are sensitive to FK506 (Bell et al. 1994). Regardless of the potential role of FKBP-type proteins as parasite virulence factors, the many critical biologically functions dependent on FKBP-type proteins makes this super-family of proteins good drug targets (Moro et al. 1995; Alag et al. 2010).

The most common parasitic protist in the United States is *Giardia lamblia* (Krappus et al. 1994): the etiological agent responsible for giardiasis, an infection of the small intestines that often causes diarrhea. While giardiasis is generally not life-threatening, in developing countries this enteric protozoan parasite contributes to malnutrition and underperformance in school, and consequently, has been added to the "Neglected Disease Initiative" list by the World Health Organization (Savioli et al. 2006). Recently, the *G. lamblia* genome was sequenced (Morrison et al. 2007) and among the 6,470 genes encoded in the five chromosomes is a putative, 109-residue FKBP-type PPIase, *Gl*-FKBP. To assist structure-based design of a more palatable, single-dose treatment for giardiasis targeting *Gl*-FKBP, we used NMR-based methods to determine its structure in solution. The structure of *Gl*-FKBP and the

G. W. Buchko · S. N. Hewitt · W. C. Van Voorhis · P. J. Myler
Seattle Structural Genomics Center for Infectious Disease, Seattle, WA, USA

G. W. Buchko (✉)
Biological Sciences Division, Biochemistry and Structural Biology, Pacific Northwest National Laboratory, Richland, WA 99352, USA
e-mail: garry.buchko@pnnl.gov

S. N. Hewitt · W. C. Van Voorhis
Department of Medicine, University of Washington, Seattle, WA 98185-7185, USA

P. J. Myler
Seattle Biomedical Research Institute, Seattle, WA 98109-5219, USA

P. J. Myler
Department of Biomedical Informatics and Medical Education, University of Washington, Seattle, WA 98195, USA

P. J. Myler
Department of Global Health, University of Washington, Seattle, WA 98195, USA

amide chemical shift assignments presented here will enable relaxation dynamics and chemical shift perturbation studies to identify and map new ligand binding surfaces on the protein (Buchko et al. 1999; Zuiderweg 2002).

## Methods and results

### Cloning, expression, and purification

The Gl-*FKBP* gene (GL50803_10450) was PCR amplified using the genomic DNA of *G. lamblia* (strain ATCC 50803/WB clone 6) and the oligonucleotide primers 5′-GGGTCCTGGTTCGATGTCGGCTCAGCTGGAGAAGA-3′ (forward) and 5′-CTTGTTCGTGCTGTTTATTAGACAGC GAGAAGCTCTACCTCA-3′ (reverse) (Invitrogen, Carlsbad, CA) containing LIC primers (underlined). This amplified Gl-*FKBP* gene was then inserted into the *NruI*/*PmeI*-digested expression vector AVA0421 by ligation-independent cloning such that the expressed gene product contained a 21 amino acid extension, MAHHHHHHMGTLEAQTGPGS-, at the N-terminus of the native protein to enable protein purification by metal chelation chromatography (Choi et al. 2011). The recombinant plasmid was then transformed into *Escherichia coli* BL21(DE3)-R3-pRARE2 cells (a gift from SGC-Toronto, Ontario, Canada) by a heat shock method. Uniformly $^{15}$N-, $^{13}$C-labeled *Gl*-FKBP was obtained by growing the transformed cells (310 K) in 750 mL of minimal medium (Miller) containing $^{15}NH_4Cl$ (1 mg/mL) and D-[$^{13}C_6$]glucose (2.0 mg/mL), NaCl (50 μg/mL), $MgSO_4$ (120 μg/mL), $CaCl_2$ (11 μg/mL), $Fe_2Cl_3$ (10 ng/mL) and the antibiotics chloramphenicol (35 μg/mL) and ampicillin (100 μg/mL). When the cell culture reached an $OD_{600}$ reading of ~0.8, it was transferred to a 298 K incubator and protein expression induced with isopropyl β-D-1-thiogalactopyranoside (0.026 μg/mL). Cells were harvested by mild centrifugation approximately 4 h later and frozen at 193 K. After thawing the frozen pellet, *Gl*-FKBP was purified with a conventional two-step protocol involving metal chelate affinity chromatography on a 20 mL Ni-Agarose 6 FastFlow column (GE Healthcare, Piscataway, NJ) followed by gel-filtration chromatography on a Superdex75 HiLoad 26/60 column (GE Healthcare, Piscataway, NJ). In addition to removing minor impurities, the latter step exchanged *Gl*-FKBP into the buffer used for the NMR studies: 100 mM NaCl, 20 mM Tris, 1.0 mM dithiothreitol, pH 7.1.

### Nuclear magnetic resonance spectroscopy

All NMR data were collected at 293 K on a double-labeled ($^{13}$C, $^{15}$N) sample of *Gl*-FKBP (~ 1.0 mM) using Varian Inova-600 and -750 spectrometers equipped with an HCN-probe and pulse field gradients. The $^{1}$H, $^{13}$C, and $^{15}$N chemical shifts of the backbone and side chain resonances were assigned from the analysis of two-dimensional $^{1}$H-$^{15}$N HSQC, $^{1}$H-$^{13}$C HSQC, HBCBCGCDHD, and HBCBCGCDCHE spectra and three-dimensional HNCACB, CBCA(CO)NH, HCC-TOCSY-NNH, CC-TOCSY-NNH, and HNCO spectra collected with Varian Biopack pulse programs. Three-dimensional $^{15}$N-edited NOESY-HSQC and $^{13}$C-edited NOESY-HSQC (aliphathic and aromatic) spectra, collected with a mixing time of 85 ms, were analyzed to obtain the side chain $^{1}$H assignments and the NOE-based distance restraints required for the structure calculations. Slowly exchanging amides were identified by lyophilizing a $^{15}$N-labeled NMR sample, re-dissolving in 99.8 % $D_2O$, and quickly collecting a $^{1}$H-$^{15}$N HSQC spectrum (~10 min later). An overall rotational correlation time, $\tau_c$, was estimated for *Gl*-FKBP from the ratio of collective backbone amide $^{15}$N $T_1$ and $T_{1\rho}$ measurements (Szyperski et al. 2002). All NMR data were processed using Felix2007 (MSI, San Diego, CA) software and analyzed with the program Sparky (v3.115). The $^{1}$H, $^{13}$C, and $^{15}$N chemical shifts were referenced using indirect methods (DSS = 0 ppm) and deposited into the BioMagResBank database (www.bmrb.wisc.edu) under the accession number BMRB-17818.

### Structure calculations

The $^{1}$H, $^{13}$C, and $^{15}$N chemical shift assignments and peak-picked NOESY data were used as initial experimental inputs in iterative structure calculations with the program CYANA (v 2.1). The assigned chemical shifts were also the primary basis for the early introduction of 75 dihedral Psi (Ψ) and Phi (Φ) angle restraints identified with the program TALOS. Towards the end of the iterative structure calculation process, 76 hydrogen bond restraints (1.8–2.0 and 2.7–3.0 Å for the NH–O and N–O distances, respectively) were introduced on the basis of proximity in early structure calculations and the observation of slowly exchanging amides in a deuterium exchange experiment. The final ensemble of 20 CYANA derived structures were then refined with explicit water with CNS (version 1.1) using the PARAM19 force field and force constants of 500, 500, and 1,000 kcal for the NOE, hydrogen bond, and dihedral restraints, respectively. For these water refinement calculations the upper boundary of the CYANA distance restraints was left unchanged and the lower boundary set to the vdw limit. Structural quality was assessed using the online Protein Structure Validation Suite (PSVS, v1.3) (Bhattacharjya et al. 2007). The structural statistics are summarized in Table 1. The atomic coordinates for the final ensemble of 20 structures for *Gl*-FKBP have been deposited in the Research Collaboratory for Structural Bioinformatics (RCSB) under PDB code 2LGO. Note that while the protein sequence in the BMRB and PDB is numbered continuously, M1–V130, starting with the 21

**Table 1** Summary of the structural statistics for *Gl*-FKBP[a]

| | |
|---|---|
| Restraints for structure calculations | |
| Total NOEs | 1,663 |
| Intraresidue NOEs | 395 |
| Sequential (i, i + 1) NOEs | 468 |
| Medium-range (i, i + j; 1 < j ≤ 4) NOEs | 251 |
| Long-range (i, i + j; j > 4) NOEs | 549 |
| Phi (Φ) angle restraints | 75 |
| Psi (Ψ) angle restraints | 75 |
| Hydrogen bond restraints | 76 |
| Structure calculations | |
| Number of structures calculated | 100 |
| Number of structures used in ensemble | 20 |
| Structures with restraint violations | |
| Distance restraint violations >0.05 Å | 0 |
| Dihedral restraint violation >1° | 0 |
| RMSD to Mean (Å) | |
| Residues: A3–R88, P91–A108 | |
| Backbone N–$C^{\alpha}$–C=O Atoms | 0.69 ± 0.08 Å |
| All heavy atoms | 1.14 ± 0.07 Å |
| Ramachandran Plots Summary for | |
| Residues A3–R88, P91–A108 using Procheck | |
| Most favored regions (%) | 92.6 |
| Additionally allowed regions (%) | 7.4 |
| Generously favored regions (%) | 0 |
| Disallowed (%) | 0 |
| Global quality scores residues A3–R88, P91–A108 | Z-score (Raw) |
| Procheck (all) | −2.42 (−0.41) |
| Procheck (Φ, Ψ) | −1.69 (−0.51) |
| MolProbity clash score | −2.07 (20.94) |

[a] All statistics are for the 20-structure ensemble deposited in the Protein Data Bank (2LGO) using the residues containing the central core (A3–R88, P91–A108)

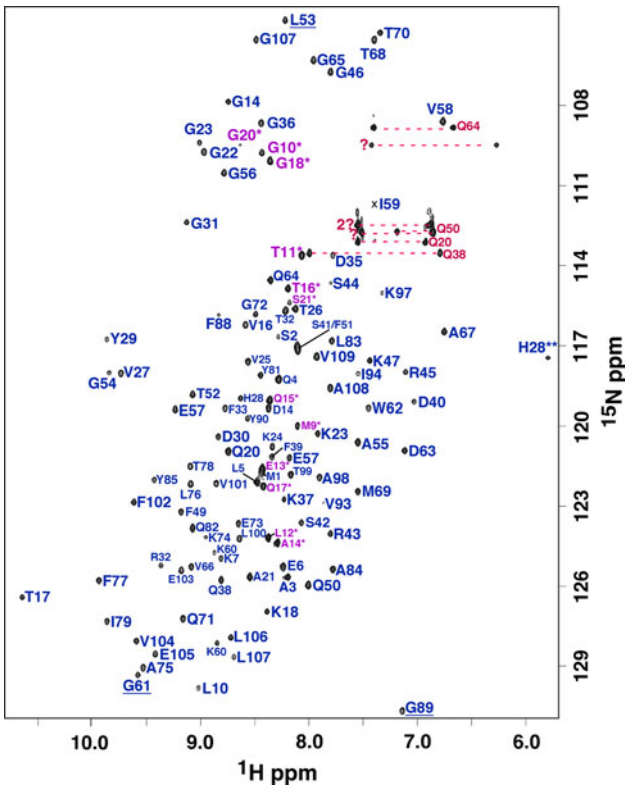


**Fig. 1** Assigned $^1$H-$^{15}$N HSQC spectrum of $^{13}$C-,$^{15}$N-labelled *Gl*-FKBP (~1.0 mM) collected at a proton resonance frequency of 750 MHz, 293 K, in 100 mM NaCl, 20 mM Tris, 1 mM DTT, pH 7.1. Amide cross peaks for the 21-residue tag (M1*-S21*) and the 109-residue native protein (M1-V109) are *colored magenta* and *blue*, respectively, with the assigned side chain resonances labeled and identified with a *red horizontal line*. Side chain cross peaks that cannot be unambiguously identified are labeled with a *red question mark*. The cross peaks for L53, G62, and G89 (*underlined*) are folded into the spectrum and the imidazole ring cross peak for H49 is indicated with a *double-asterisk*

residues of the non-native N-terminal tag, here, the non-native residues of the N-terminal tag are labeled with an asterisk (M1*–S21*) and the first native residue (M22 in the BMRB and PDB sequence) is numbered M1 without an asterisk.

## Solution structure of *Gl*-FKBP

Recombinant *Gl*-FKBP has a molecular weight of 14.2 kDa (including the 21-residue N-terminal tag). Behavior of the protein on a size exclusion chromatography column and in NMR spectroscopy experiments indicated that *Gl*-FKBP was a monomer in solution. First, under a flow rate of 2.5 mL/min, *Gl*-FKBP eluted off a 26/60 Superdex75 size exclusion column with a retention time (90 min) characteristic of an ~14 kDa protein (data not shown). Second, the estimated isotropic overall rotational correlation time ($\tau_c$) inferred from $^{15}$N spin relaxation times (Szyperski et al. 2002) was 10.6 ± 0.6 ns at 293 K, a value most consistent with an ~14 kDa protein. Third, there was good magnetization transfer in all the three-dimensional backbone NMR experiments, an unlikely observation if *Gl*-FKBP formed dimers or higher order oligomers.

The $^1$H-$^{15}$N HSQC spectrum for *Gl*-FKBP is illustrated in Fig. 1. The good chemical shift dispersion of the amide resonances in both the $^1$H and $^{15}$N dimension is characteristic of a folded protein and facilitated spectral assignments. All the visible backbone amide resonances were identified with the labeled assignments colored magenta and blue in Fig. 1 for the non-native (M1*–S21*) and native (M1–V109) residues, respectively. Amide cross peak were not visible for the N-terminal eight residues of the tag and E108. The side chain $NH_2$ groups, labeled with red dashed lines in Fig. 1, were unambiguously identified for four out of the eight glutamine residues. The unassigned

pairs are labeled with a question mark and three out of the four (Q15*, Q17*, and Q4) belong to residues in, or near, the non-native N-terminal tag. While all the non-exchangeable ring protons for the lone tryptophan residue (W62) were assigned, there was no evidence for its side chain amide cross peak in the $^{1}H$-$^{15}N$ HSQC spectrum. Interestingly, W62 is a highly conserved residue in FKBP-type proteins and makes direct contact with FK506 in co-crystal structures (Chakraborty et al. 2012). Given the observation of 110 out of the 119 possible backbone amide resonances ((130−(10 Pro + M1)), 92 %) in the $^{1}H$-$^{15}N$ HSQC spectrum for *Gl*-FKBP and the complete assignment of these observed resonances, it was possible to assign over 90 % of the backbone and side chain carbon and proton resonances for residues M9*–V109.

The extensive assignment of the backbone and side chain $^{1}H$, $^{13}C$, and $^{15}N$ chemical shifts for *Gl*-FKBP were crucial initial experimental inputs for the automatic assignment of the peak-picked NOESY data in iterative structure calculations with the program CYANA. As summarized in the structure statistics table (Table 1), 1663 NOESY peaks were assigned in the final round of structure calculations that also included 76 hydrogen bond distance restraints and 150 total Psi and Phi torsion angle restraints. Each member of the final ensemble of 20 structures satisfied the experimental data with no upper limit distance violation >0.05 Å and no torsion-angle violation >1.0°. Ensemble analysis with the PSVS validation-software package further confirmed a quality set of final structures (Bhattacharjya et al. 2007). Ramachandran statistics for the Phi/Psi pairs of all the residues in the ensemble were overwhelmingly in acceptable space (92.6 % most favored regions and 7.4 % additionally allowed regions) and all the structure-quality Z-scores were acceptable (>−5). Figure 2a is a superposition of the ordered regions of the final ensemble of 20 calculated structures upon the average structure and visually shows that the final ensemble of calculated structures converge well. The good convergence is expressed mathematically in Table 1. The RMSD of the structured core (A3–R88, P91–A108) of the ensemble from the mean structure is 0.69 ± 0.08 Å for the backbone atoms (N–$C^{\alpha}$–C=O) and 1.14 ± 0.07 Å for all heavy atoms.

Figure 2b is a cartoon representation of the structure of *Gl*-FKBP (structure closest to the average in the ensemble shown in Fig. 2a) and Fig. 2c is a two-dimensional schematic of the individual secondary structure components. The protein is composed of an α-helix (I59–M69) nestled along the face of a six-strand antiparallel β-sheet, β3/β4-β2-β6-β5-β1. Two short β-strands, β3 (Q38-D40) and β4 (F49-F51), are hydrogen bonded along one side of β2 (V25–R32) to form one end of the β-sheet. Beta-2 forms hydrogen bonds with the central β-strand, β6 (L100–A108), and β6 forms hydrogen bonds with β5 (E73–I79) on its opposite side.

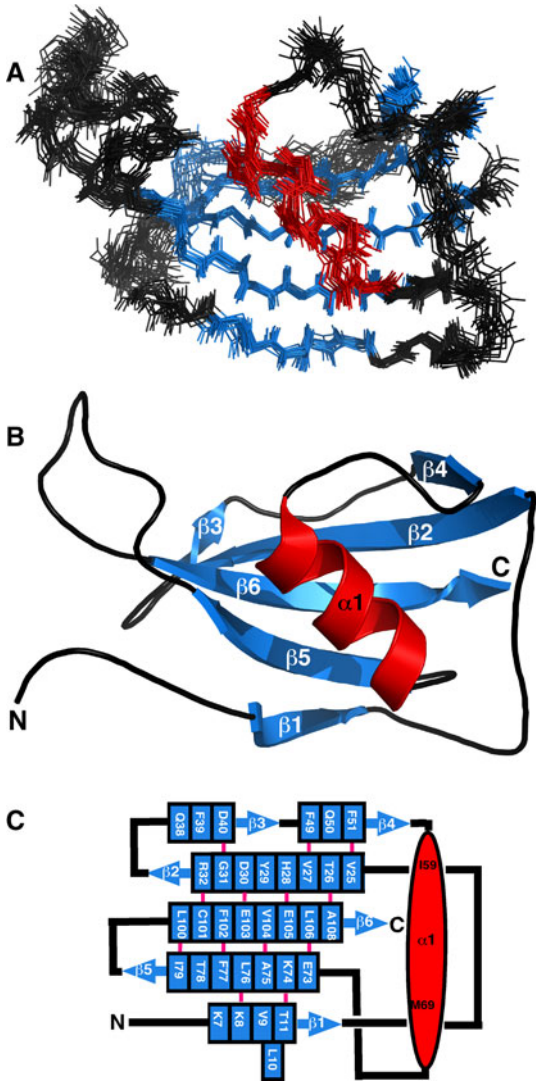


**Fig. 2** **a** Backbone superposition of the ensemble of 20 structures calculated for *Gl*-FKBP on the structure closest to the average. The 21-residue N-terminal tag has been removed for clarity. **b** Cartoon representation of the structure closest to the average structure. The β-strands and α-helix are colored *marine* and *red*, respectively. **c** Secondary-structure diagram for *Gl*-FKBP. The α-helix is illustrated as a *red oval* and the β-strands as *solid marine arrows* with individual amino acids enclosed in individual boxes. A *solid pink line* between β-strand residues indicates a backbone hydrogen bond pair between two residues in an antiparallel β-sheet. Bulges in the β-sheet are present at residues L10 and L107 (the latter one is not illustrated in the Fig.). The *black lines* connecting secondary structure elements are not drawn to scale

Beta-6 is interrupted by a single residue β-bulge at L107. Capping the other end of the β-sheet is β1 (K7–T11) that contains a single residue β-bulge at L10 and forms hydrogen bonds with β5. Overall, the half-β-barrel/helix structure is similar to the fold observed in crystal and NMR-derived structures of other proteins in the FKBP super-family (Liang et al. 1996; Burkhard et al. 2000; Kotaka et al. 2008; Alag et al. 2010; Chakraborty et al. 2012).

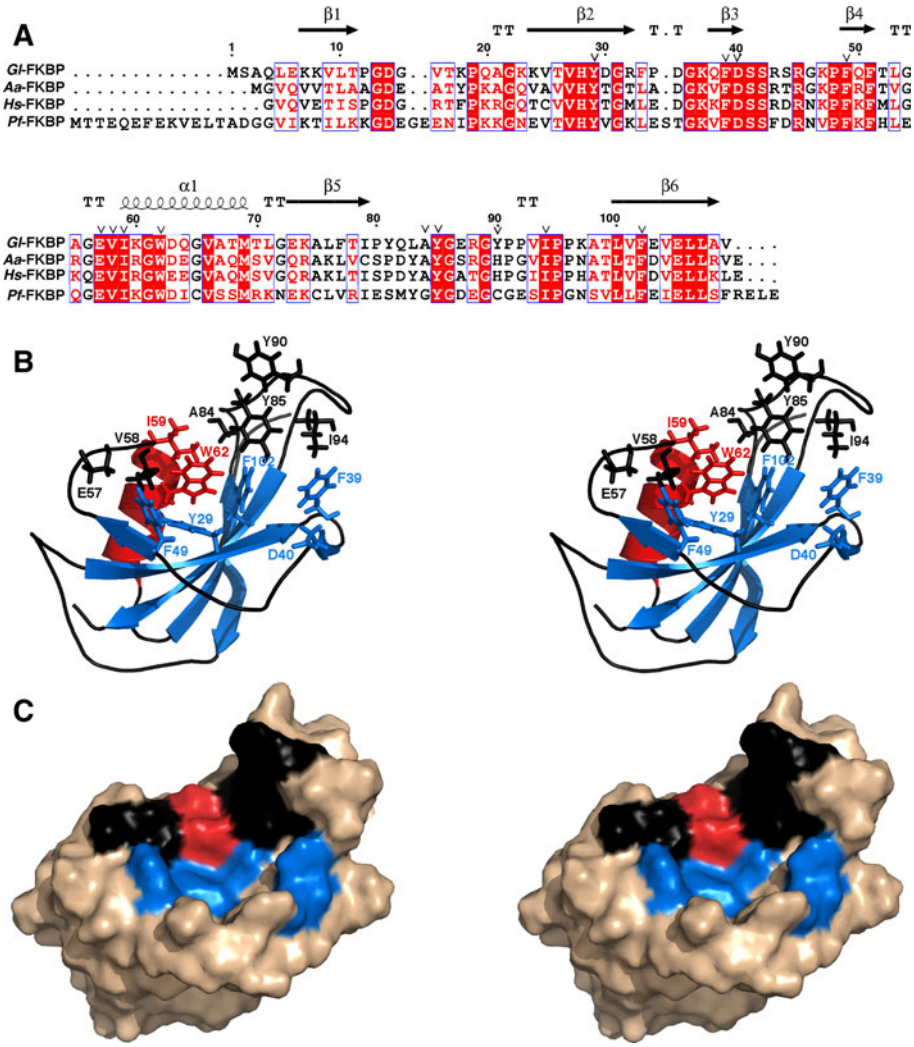


**Fig. 3** **a** ClustalW2 multiple amino acid sequence alignment of *Gl*-FKBP with FKBP or a FKBP domain from *Aedes aegypti* (*Aa*-FKBP), *Homo sapiens* (*Hs*-FKBP) and *P. falciparum* (*Pf*-FKBP) illustrated with ESPript (Gouet et al. 1999). *Red shaded regions* highlight invariant residues and *red* residues highlight conserved residues in the alignment. *Pf*-FKBP residues observed to interact with the immunosuppresive drug FK506 in a complex crystal structure (2VN1) (Kotaka et al. 2008) are indicated by an open triangle above the *Gl*-FKBP sequence. The elements of secondary structure observed for *Gl*-FKBP are illustrated above the alignment. **b** Stereo-view highlighting the side chains of the equivalent residues in the solution structure of *Gl*-FKBP that are predicted to make contact with FK506 based on the interactions observed in the *Pf*-FKBP-FK506 crystal structure (*inverted triangles* in (**a**)). The structure closest to the average is shown with the β-strands, loops/turns, and α-helix colored *marine*, *black*, and *red*, respectively. **c** Stereo-view of the solvent accessible surface rendition of **b** highlighting the predicted FK506 binding surface on the solution structure of *Gl*-FKBP

## Discussion and conclusions

Figure 3a is a ClustalW alignment (Larkin et al. 2007) of the amino acids sequence of *Gl*-FKBP with (1) the FK506 binding protein FKBP12 from *Aedes aegypti* (*Aa*-FKBP), the yellow fever mosquito that acts as the vector for dengue fever and other diseases (Chakraborty et al. 2012), (2) the C-terminal, FK506 binding domain of human FKBP12 (*Hs*-FKBP) (Liang et al. 1996), and (3) the N-terminal, FK506 binding domain of FKBP35 from *P. falciparum* (*Pf*-FKBP), the protozoan parasite responsible for malaria (Kotaka et al. 2008). The sequence identity between *Gl*-FKBP and the other three sequences are: *Pf*-FKBP = 44 %, *Hs*-FKBP = 55 %, and *Aa*-FKBP = 57 %. Structures have been determined for all four aligned proteins and, despite the moderate sequence identity, the backbone Cα RMSD between *Gl*-FKBP and the other three apo structures indicate the adoption of a similar fold: *Pf*-FKBP (2OFN) = 2.9 Å, *Hs*-FKBP (2PPN) = 2.2 Å, and *Aa*-FKBP (2LPV) = 1.8 Å (Holm and Rosenström 2010). The residues observed to interact with FK506 in a co-crystal structure with *Pf*-FKBP (2VN1) (Kotaka et al. 2008) are indicated by an open triangle above the *Gl*-FKBP sequence in Fig. 3a. The side chains of these equivalent residues in *Gl*-FKBP are highlighted in the stereo-views in Fig. 3b and c. These views show that all

these residues lie together on the same face of the protein and are, for the most part, accessible to the solvent, suggesting that it is likely that FK506 will also bind to this region on *Gl*-FKBP. Note that while the majority of the residues in *Ps*-FKBP that interact with FK506 are in conserved regions, two non-conserved residues that interact with FK506 are in the loop between β5 and β6 (A84 and Y90 in *Gl*-FKBP). There are also two conserved residues in the loop between β4 and the α-helix in *Gl*-FKBP (E57 and V58) that interact with FK506 that are adjacent to a non-conserved residue (G56 in *Gl*-FKBP versus Q56 in *Hs*-FKBP). These two loop regions "bookend" the putative FK506 binding site (black region in Fig. 3c) and also have some sequence variability and may be potential regions to exploit in the discovery of novel drugs that bind to *Gl*-FKBP but not *Hs*-FKBP (Kotaka et al. 2008).

In summary, the $^{1}$H, $^{13}$C, and $^{15}$N chemicals shifts have been extensively assigned for *Gl*-FKBP, a 109-residue, FKBP-type, peptidyl-proline *cis–trans* isomerase from *G. lamblia*. These chemical shift assignments were deposited into the BioMagResBank database under the accession number BMRB-17818 and used in the determination of the solution structure for *Gl*-FKBP (PDB-ID 2LGO). *Gl*-FKBP adopts the cononical fold observed for other FKBP structures with the core consisting of an α-helix (I59–M69) nestled against the face of a six-strand, antiparallel β-sheet (β3/β4-β2-β6-β5-β1). The combination of an assigned $^{1}$H-$^{15}$N HSQC spectrum and solution structure for *Gl*-FKBP will enable chemical shift perturbation and backbone dynamics studies and assist in the identification and characterization of ligand binding surfaces on the protein (Buchko et al. 1999; Zuiderweg 2002; Alag et al. 2010). Such experiments will accelerate efforts towards exploiting FKBP-type proteins as antimicrobial drug targets and the generation of new intervention strategies to treat and control giardiasis (Myler et al. 2009).

**Acknowledgments** Funding for this research was provided by the National Institute of Allergy and Infectious Diseases, National Institute of Health, Department of Health and Human Services, under Federal Contract numbers HHSN272201200025C and HHSN272200700057C. The SSGCID internal ID for *Gl*-FKBP is GilaA.00840.a. Much of this research was performed at the W.R. Wiley Environmental Molecular Sciences Laboratory (EMSL), a national scientific user facility located at Pacific Northwest National Laboratory (PNNL) and sponsored by U.S. Department of Energy's Office of Biological and Environmental Research (BER) program. Battelle operates PNNL for the U.S. Department of Energy.

## References

Alag R, Qureshi IA, Bharatham N, Shin J, Lescar J, Yoon HS (2010) NMR and crystallographic structures of the FK506 binding domain of human malarial parasite *Plasmodium vivax* FKBP35. Protein Sci 19(8):1577–1586

Bell A, Wernli B, Franklin RM (1994) Roles of peptidyl-prolyl *cis–trans* isomerase and calcineurin in the mechanisms of antimalarial action of cyclosporin A, FK506, and rapamycin. Biochem Pharmacol 48(3):495–503

Bhattacharjya S, Tejero R, Montelione GT (2007) Evaluating protein structures determined by structural genomics consortia. Proteins 66(4):778–795

Buchko GW, Daughdrill GW, de Lorimier R, Rao S, Isern NG, Lingbeck J, Taylor J-S, Wold MS, Gochin M, Spicer LD, Lowry DF, Kennedy MA (1999) Interactions of human nucleotide excision repair protein XPA with DNA and RPA70ΔC327: chemical shift mapping and $^{15}$N NMR relaxation studies. Biochemistry 38(46):15116–15128

Burkhard P, Taylor P, Walkinshaw MD (2000) X-ray structure of small ligand-FKBP complexes provide an estimate for hydrophobic interaction energies. J Mol Biol 295(4):953–962

Chakraborty G, Shin J, Nguyen QT, Harikishore A, Baek K, Yoon HS (2012) Solution structure of FK5606-binding protein 12 from *Aedes aegypti*. Proteins 80:2476–2481

Choi R, Kelly A, Hewitt SN, Napuli AJ, Van Voorhis WC (2011) Immobilized metal-affinity chromatography protein-recovery screening is predictive of crystallograhic structure success. Acta Cryst F67(9):998–1005

Göthel SF, Marahiel MA (1999) Peptidyl-propyl *cis–trans* isomerases, a superfamily of ubiquitous folding catalysts. Cell Mol Life Sci 55(3):423–436

Gouet P, Courcelle E, Stuart DI, Metoz F (1999) ESPript: analysis of multiple sequence alignments in postscript. Bioinformatics 15(4):305–308

Holm L, Rosenström P (2010) Dali server: conservation mapping in 3D. Nucl Acids Res 38(S2):W545–W549

Kotaka M, Ye H, Alag R, Hu G, Bozdech Z, Preiser PR, Yoon HS, Lescar J (2008) Crystal structure of the FK506 binding domain of *Plasmodium falciparum* FKBP35 in comples with FK506. Biochemistry 47(22):5951–5961

Krappus KD, Lundgren RG, Juranek DD, Roberts JM, Spencer HC (1994) Intestinal parasitism in the United States: update on a continuing problem. Am J Trop Med Hyg 50(6):705–713

Larkin MA, Blackshields G, Brown NP, Chenna R, McGettigan PA, McWilliam H, Valentin F, Wallace IM, Lopez R, Thompson JD, Gibson TJ, Higgins DG (2007) ClustalW and ClustalX version 2.0. Bioinformatics 23(21):2947–2948

Liang J, Hung DT, Schreiber SL, Clardy J (1996) Structure of the human 25 kDa binding domain protein complexed with rapamycin. J Am Chem Soc 118(5):1231–1232

Moro A, Ruiz-Cabello F, Fernández-Cano A, Stock RP, González A (1995) Secretion by *Trypanosoma cruzi* of a peptidyl-propyl *cis–trans* isomerase involved in cell infection. EMBO J 14(3):2483–2490

Morrison HG, McArthur AG, Gillin FD, Aley SB, Adam RD, Olsen GJ, Best AA, Cande WZ, Chen F, Cipriano MJ, Davids BJ, Dawson SC, Elmendorf HG, Hehl AB, Holder ME, Huse SM, Kim UU, Lasek-Nesselquist E, Manning G, Nigam A, Nixon JE, Palm D, Passamaneck NE, Prabhu A, Reich CI, Reiner DS, Samuelson J, Svard SG, Sogin ML (2007) Genomic minimalism in the early diverging intestinal parasite *Giardia lamblia*. Science 317(5846):1921–1926

Myler PJ, Stacy R, Stewart LJ, Staker BL, Van Voorhis WC, Varani G, Buchko GW (2009) The Seattle Structural Genomics Center for Infectious Disease (SSGCID). Infect Dis Drug Targets 9(5):493–506

Savioli L, Smith H, Thompson A (2006) Giardia and cryptosporidium join the "neglected diseases initiative". Trends Parasitol 22(5):203–208

Szyperski T, Yeh DC, Sukumaran DK, Moseley HNB, Montelione GT (2002) Reduced-dimensionality NMR spectroscopy for high-throughput protein resonance assignment. Proc Natl Acad Sci USA 99(12):8009–8014

Zuiderweg ERP (2002) Mapping protein–protein interactions in solution using NMR spectroscopy. Biochemistry 41(1):1–7